Nanoscale Research Letters
a SpringerOpen Journal

NANO EXPRESS Open Access

Nanoscale evidence of erbium clustering in Er-doped silicon-rich silica

Etienne Talbot[1*], Rodrigue Lardé[1], Philippe Pareige[1], Larysa Khomenkova[2], Khalil Hijazi[2] and Fabrice Gourbilleau[2]

Abstract

Photoluminescence spectroscopy and atom probe tomography were used to explore the optical activity and microstructure of Er^{3+}-doped Si-rich SiO_2 thin films fabricated by radio-frequency magnetron sputtering. The effect of post-fabrication annealing treatment on the properties of the films was investigated. The evolution of the nanoscale structure upon an annealing treatment was found to control the interrelation between the radiative recombination of the carriers via Si clusters and via 4*f* shell transitions in Er^{3+} ions. The most efficient 1.53-μm Er^{3+} photoluminescence was observed from the films submitted to low-temperature treatment ranging from 600°C to 900°C. An annealing treatment at 1,100°C, used often to form Si nanocrystallites, favors an intense emission in visible spectral range with the maximum peak at about 740 nm. Along with this, a drastic decrease of 1.53-μm Er^{3+} photoluminescence emission was detected. The atom probe results demonstrated that the clustering of Er^{3+} ions upon such high-temperature annealing treatment was the main reason. The diffusion parameters of Si and Er^{3+} ions as well as a chemical composition of different clusters were also obtained. The films annealed at 1,100°C contain pure spherical Si nanocrystallites, $ErSi_3O_6$ clusters, and free Er^{3+} ions embedded in SiO_2 host. The mean size and the density of Si nanocrystallites were found to be 1.3 ± 0.3 nm and $(3.1 \pm 0.2) \times 10^{18}$ Si nanocrystallites·cm^{-3}, respectively. The density of $ErSi_3O_6$ clusters was estimated to be $(2.0 \pm 0.2) \times 10^{18}$ clusters·cm^{-3}, keeping about 30% of the total Er^{3+} amount. These Er-rich clusters had a mean radius of about 1.5 nm and demonstrated preferable formation in the vicinity of Si nanocrystallites.

Keywords: Erbium, Silicon, Nanocrystallites, Nanoclusters, Sputtering, Atom probe tomography, Photoluminescence

Background

Silicon-based photonics is a fast growing field of semiconductor nanoscience. A part of this area focuses on the realization of integrated optoelectronic devices (such as light planar waveguide amplifier, light-emitting diodes, lasers, ...) to overcome the interconnect bottleneck for Si-based integrated circuits. In this regard, the use of optical interconnection is the most promising. Among the different strategies, the most considered for Si-based telecommunication are (1) doping of silica fibers with Er^{3+} ions which offered the emission at the standard telecommunication wavelength (1.53 μm) and (2) incorporation of quantum-confined Si nanoclusters (Si-ncs) or nanocrystallites (Si-NCs) in such doped fibers, favoring an enhancement of Er-effective excitation cross section. Both these approaches fully exploit the individual properties of Si-ncs (Si-NCs) and rare-earth ions [1,2].

It was already demonstrated that Si-nc/SiO_2 interface affects significantly not only the properties of the Si-ncs themselves, but also the optical activity of Er^{3+} ions coupled with Si-ncs [1,3,4]. It was shown that a thin 0.8-nm sub-stoichiometric interface between the Si-nc and the SiO_2 host plays a critical role in the Si-nc emission [5,6]. Furthermore, numerous studies allowed the determination of the main mechanism of the interaction between the Si-ncs and the neighboring Er^{3+} ions [1,2,7]. Along with the effect of structural environment of both Er^{3+} ions and Si-ncs on their individual properties, it has also been observed that very small Si-ncs, even amorphous, allow an efficient sensitizing effect towards Er^{3+} ions. However, the efficiency of this process depends on the separating

*Correspondence: etienne.talbot@univ-rouen.fr
[1]Groupe de Physique des Matériaux (GPM), Université et INSA de Rouen, UMR CNRS 6634, Normandie Université, Av. de l'Université, BP 12, Saint Etienne du Rouvray, 76801, France
Full list of author information is available at the end of the article

distance between Si-ncs and rare-earth ions [7-9]. Critical interaction distances were found to be about 0.5 nm [7,9,10].

In spite of the significant progress in the investigation of the excitation processes in Er-doped Si-rich SiO_2 materials, some issues are still debatable, such as the spatial location of optically active Er^{3+} ions with regard to Si-ncs. Another aspect, which may control the optical properties, is the distribution of Er dopants in the film, i.e., either these ions are uniformly distributed or they form some agglomerates [11]. Thus, mapping the Si and Er^{3+} distributions in Er-doped Si-rich SiO_2 films as well as the investigation of the evolution of these distributions versus fabrication conditions and post-fabrication processing are the key issues to manage the required light-emitting properties of such systems.

Up to now, high-resolution and energy-filtered transmission electron microscopies were the only techniques offered a direct visualization of Si and Er distributions [11-13]. Nevertheless, other indirect techniques, such as fluorescence-extended X-ray absorption fine-structure spectroscopy [14-16] or X-ray photoelectron spectroscopy [17], have evidenced that the amount of Er clusters in Er-doped Si-rich SiO_2 films depends strongly on the preparation conditions or annealing temperature. We have recently demonstrated the feasibility of atom probe tomography (APT) analysis of Si-rich SiO_2 systems, giving its atomic insight [18,19]. With the benefit of this expertise, the purpose of this paper is to perform a deep analysis of Er-doped Si-rich SiO_2 thin films by means of APT experiments to understand the link between the nanoscale structure of the films and their optical properties. The distributions of Si and Er^{3+} ions in as-grown films were investigated. The evolutions of chemical composition of the films upon annealing treatment, the formation of Si-ncs, and the redistribution of Er^{3+} ions were studied with the aim of finding the way to control the microstructure at the atomic scale and to optimize light-emitting properties of the Er-doped Si-rich SiO_2 system.

Methods

Sample fabrication

Er-doped Si-rich SiO_2 (Er-SRSO) layers were grown by radio-frequency (RF) magnetron-sputtering technique. For the APT experiments, the deposition was performed on an array of p-doped Si(100) posts (5 μm in diameter and 100 μm in height). This method, already used in previous works, allows a simple procedure for atom probe sample preparation [20]. For optical experiments, the layers were grown on standard p-type (100) Si wafers in the same deposition run. The film fabrication approach comprises the co-sputtering of Er_2O_3, SiO_2, and Si targets in pure argon plasma on substrate kept at 500°C. The Er content and the Si excess were independently controlled through the RF power applied on the corresponding cathode. More details on the fabrication processes can be found in other works [12,21]. The thickness of the Er-SRSO layer was 200 nm. The concentration of Er^{3+} ions in the sample was 1×10^{21} at./cm^3, while the Si excess was about 5 at.% [21]. To study the effect of post-fabrication treatment on structural and optical properties of the layers, each sample was divided into several parts. One of them was kept as a reference for the 'as-deposited' state. The others were submitted to an annealing treatment in conventional furnace in constant nitrogen flow to study the phase separation, the Si-nc formation, the recovering of the defects, and thus, the enhancement of Er emission. The samples were annealed at 600°C for 10 h, 900°C for 1 h, and 1,100°C for 1 h. The annealing time for each temperature corresponds to optimal conditions, giving rise to the highest photoluminescence of the Er^{3+} ions.

Atom probe tomography

Among the various analytical techniques, atom probe tomography is one of the most promising when atomic scale resolution, three-dimension reconstruction, and quantitative chemical characterization are required [22,23]. The recent improvement of this technique with the implementation of femtosecond laser pulses [24] allowed to enlarge the variety of materials to be studied. Thus, an atomic observation of photonic, solar cells, magnetic semiconductor, or nanoelectronic devices is now available [18,19,25-28]. The Er-SRSO film with the shape of a tiny needle, required for APT analyses, was prepared using a focused ion beam annular milling procedure. The details of this standard procedure are reported in another work [20]. In order to prevent the layer of interest from Ga damages and/or amorphization during the sample processing, a 300-nm-thick layer of Cr was pre-deposited on the top of the sample. Films were then ion-milled into sharp tips with an end radius close to 30 nm. A low-accelerating voltage (2 kV) was used for the final stage in order to avoid Ga implantation and sample amorphization. The APT used in this work is the CAMECA (CAMECA SAS, Gennevilliers Cedex, France) laser-assisted wide-angle tomographic atom probe. The experiments were performed with samples cooled down to 80 K, with a vacuum of (2 to 3) $\times$ 10^{-10} mbar in the analysis chamber and with ultraviolet ($\lambda = 343$ nm) femtosecond (350 fs) laser pulses. The laser energy was fixed at 50 nJ/pulse focused onto an approximately 0.01-mm^2 spot.

To identify the clusters, the algorithm described hereafter was applied. Each step of this identification comprises the placement of a sphere (sampling volume) over one atom of the volume investigated and the estimation of the local composition of the selected elements by counting

atoms within this sphere. If the composition exceeds a given threshold, the atom at the center of the sphere is associated to a cluster. If the composition is lower than the threshold, the atom at the center of the sphere belongs to the matrix. The sphere is then moved to the next atom, and this procedure is applied again to estimate the composition and to compare it with the threshold value. This approach was used for all the atoms of the volume to identify those belonging either to the clusters or to the matrix. In this paper, a threshold of 75% of Si and 5% of Er was used to identify pure Si nanoclusters and Er-rich regions with a sphere radius of 1 nm.

Photoluminescence study

The photoluminescence (PL) properties of the samples were examined using the 476-nm excitation line delivered by an Innova 90C coherent Ar^+ laser (Coherent Inc., Santa Clara, CA, USA). The pumping at 476 nm, which is nonresonant for Er^{3+} ions, was always used to ensure that Er^{3+} excitation was mediated by the Si-based sensitizers. The Er^{3+} PL spectra in the 1.3- to 1.7-μm spectral range were measured at room temperature by means of a Jobin Yvon (HORIBA Jobin Yvon Inc., Edison, NJ, USA) 1-m single-grating monochromator coupled to a North Coast germanium detector (North Coast Scientific Co., Santa Rosa, CA, USA) cooled with liquid nitrogen. The Si-nc PL properties were investigated in the 550- to 1,150-nm spectral range using a Triax 180 Jobin Yvon monochromator with an R5108 Hamamatsu PMT (HAMAMATSU PHOTONICS DEUTSCHLAND GmbH, Herrsching am Ammersee, Germany). The PL signal was recorded in both cases through an SRS lock-in amplifier (SP830 DPS; Stanford Research Systems, Inc., Sunnyvale, CA, USA) referenced to the chopping frequency of light of 9.6 Hz. All PL spectra were corrected on the spectral response of experimental setup.

Results and discussion

Photoluminescence spectra

The PL spectra, recorded on the as-deposited layer and after different annealing treatments, are reported in Figure 1. The highest PL intensity in the 500- to 950-nm spectral range is detected for the sample annealed at 1,100°C for 1 h (Figure 1a). This PL band is a feature of Si-ncs, which confirmed the Si-nc formation in our sample similar to the results of another work [21]. In the infrared spectral range (1.4 to 1.6 μm), the highest Er^{3+} PL efficiency was obtained for the sample annealed at 600°C (Figure 1b). Meanwhile, the increase of annealing temperature from 600°C to 900°C results in the slight decrease of the Er^{3+} PL emission. Further temperature rise from 900°C to 1,100°C leads to a decrease of the PL intensity by a factor of 10 (Figure 1b). By comparison, the PL efficiency at 1.53 μm of the as-deposited layer is slightly higher than that observed for 1,100°C annealed sample. Based on previous results [12,13], this behavior of Er^{3+} emission in as-deposited layer suggests that Si sensitizers are already formed, allowed by the relatively high deposition temperature (500°C). Another argument for Si-nc formation is the absence of Er^{3+} emission in Er-doped SiO_2 counterparts submitted to the same annealing treatment. To explain the lowering of the Er^{3+} PL intensity after 1,100°C annealing, APT experiments have been performed on the as-deposited and 1,100°C annealed samples.

Atom probe experiments

Prior to the study of microstructure, chemical analysis of the samples was performed by means of the APT technique. A typical mass spectrum of Er-SRSO layers is shown in Figure 2. The mass-over-charge ratio is a characteristic of the chemical nature of each ion collected during atom probe analysis. The presence of the three chemical elements (Si, O, and Er), constituting our samples, is clearly seen (Figure 2). Silicon is identified, after field evaporation, in three different charged states: Si^{3+}, Si^{2+}, and Si^{1+}. The three isotopes of silicon are detected to be in good agreement with their respective relative natural abundances (Figure 2a). The oxygen is found as molecular ions O_2^{2+} and O_2^{1+} (Figure 2a). Finally, erbium ions are mostly detected as Er^{3+} or Er^{2+} (Figure 2b). The composition deduced from the mass spectrum of the as-grown and annealed samples is presented in Table 1. No significant difference of the overall composition can be seen for both samples analyzed. The Er content, measured as approximately 1.0×10^{21} at/cm^3, is in agreement with that expected from fabrication conditions [29].

Figure 3 shows the 3D distributions of Si, O, and Er atoms within the reconstructed volume obtained from the APT analysis of the as-deposited layer where each dot corresponds to one atom detected. Statistical treatment of APT data was used to quantify concentration fluctuations in the sample. Frequency distribution was compared to binomial distribution to evidence the phase separation and atom clustering. This treatment performed on as-deposited material indicates a homogeneous spatial distribution of the three chemical species (Si, O, and Er) in the analyzed volume ($41 \times 41 \times 88$ nm^3). Thus, it suggests that no Er clustering occurs during the deposition process. Moreover, it is worth to note that, based on these frequency distributions, we estimate that Si-ncs or Er clusters with a diameter below 0.8 nm (corresponding to agglomerated 15 Si atoms or 10 Er atoms) could not be distinguished from free Si or Er atoms. These atomic scale investigations, correlated with the PL data (Figure 1), suggest that in the as-deposited sample, the Si sensitizers consist of less than 15 Si atoms and are efficient to excite neighboring Er^{3+} ions.

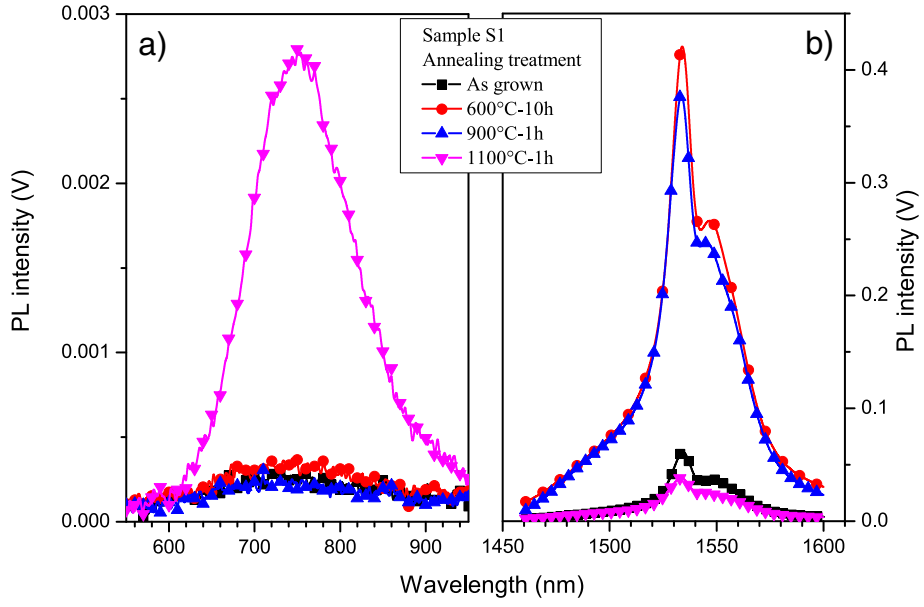

Figure 1 Photoluminescence spectra. Photoluminescence spectra of the sample detected for as-grown and annealed samples in (**a**) visible spectral range (500 to 950 nm) and (**b**) infrared spectral range (1.4 to 1.6 μm). The experiments have been carried out using the 476.5-nm wavelength (nonresonant excitation for Er^{3+} ions).

Before 2003 [13], the standard annealing treatment, applied for the formation of Si-NCs in Si-rich SiO_2 materials fabricated by different approaches, was an annealing at 1,100°C for 1 h in pure nitrogen gas. The same annealing treatment was considered to be efficient to create the Si-NCs in Er-doped Si-rich SiO_2 materials to achieve a sensitizing effect towards rare-earth ions. Figure 4 shows the 3D cluster-filtered distribution of chemical species in the Er-SRSO layers submitted to such thermal treatment. The Si-ncs are clearly seen; their density is estimated to be about $(3.1 \pm 0.2) \times 10^{18}$ Si-ncs/cm^3. The mean distance between Si-ncs, derived from their density, is found to be 6.9 ± 0.2 nm, which is in agreement with that deduced from the 3D reconstruction. The Si-ncs are spherical in shape and are homogeneously distributed in the analyzed volume. Simultaneously, a large density of Er-rich clusters approximately (2.0×10^{18} Er-NCs/cm^3) has also been detected in the sample (Figure 4). Furthermore,

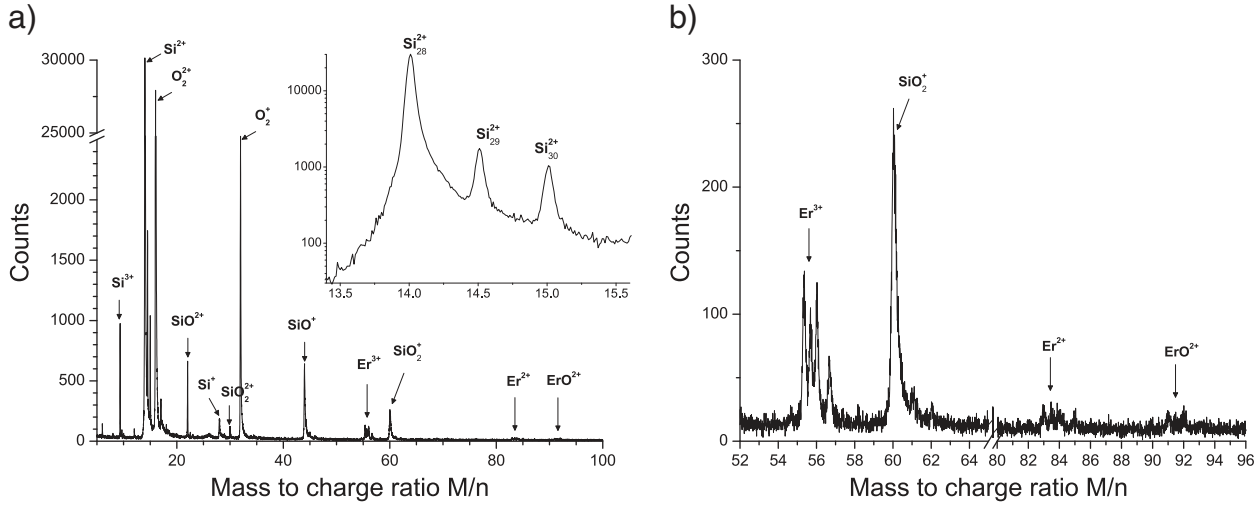

Figure 2 Atom probe mass spectrum. APT mass spectrum obtained on Er-doped Si-rich SiO_2 sample. (**a**) Typical mass spectrum with Si, O, and Er identified peaks. Isotopes of silicon for the Si^{2+} peak are evidenced in the inset. (**b**) Magnification of the Er peaks in the 52- to 96-M/n region.

Table 1 APT compositions of the Er-doped SRSO layer in the as-deposited and 1,100°C 1-h annealed state

	As-deposited	Annealed at 1,100°C
Si (at.%)	35.1 ± 0.4	35.0 ± 0.4
O (at.%)	63.2 ± 0.4	63.1 ± 0.4
Er (at.%)	1.7 ± 0.4	1.9 ± 0.4
Er (at·cm^{-3})	1.1 × 10^{21}	1.3 × 10^{21}
Si excess (at.%)	Approximately 3.6 %	Approximately 3.5%

some Si-ncs are interconnected by Er clusters (or channel) as illustrated in the inset of Figure 4. No particular morphology of these Er clusters has been deduced.

This result shows that thermal treatment at 1,100°C leads to a formation of a three-phase system: silica matrix, Si-ncs, and Er-rich clusters. The formation of such Er clusters is accompanied by the enlargement of the distance between Si-ncs, and it explains why annealing at 1,100°C quenches the PL emission with respect to the lower annealing treatments. Although the formation of Si-ncs increases the probability of absorbing excitation

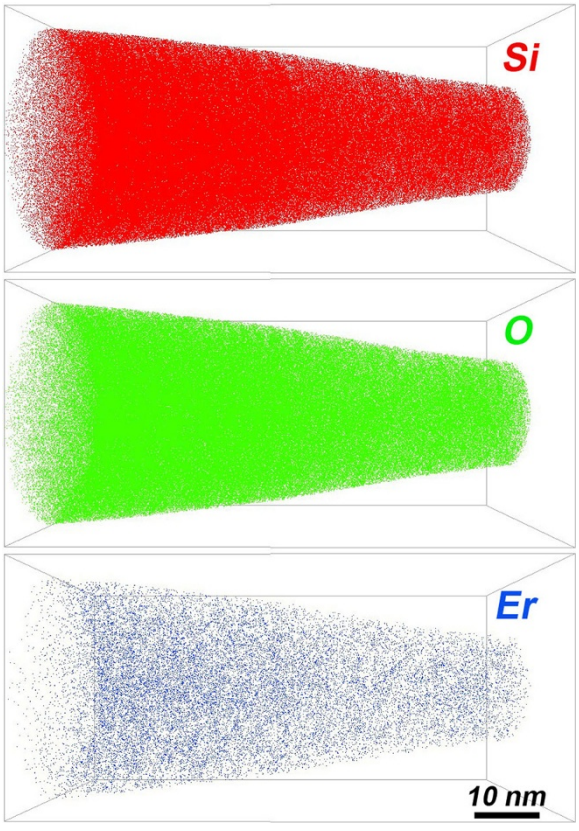

Figure 3 3D reconstruction of the as-grown Er-doped SRSO layers of APT analysis. APT reconstruction of 3D distribution of silicon, oxygen, and erbium atoms in the as-grown sample. The volume analyzed is 41 × 41 × 88 nm^3.

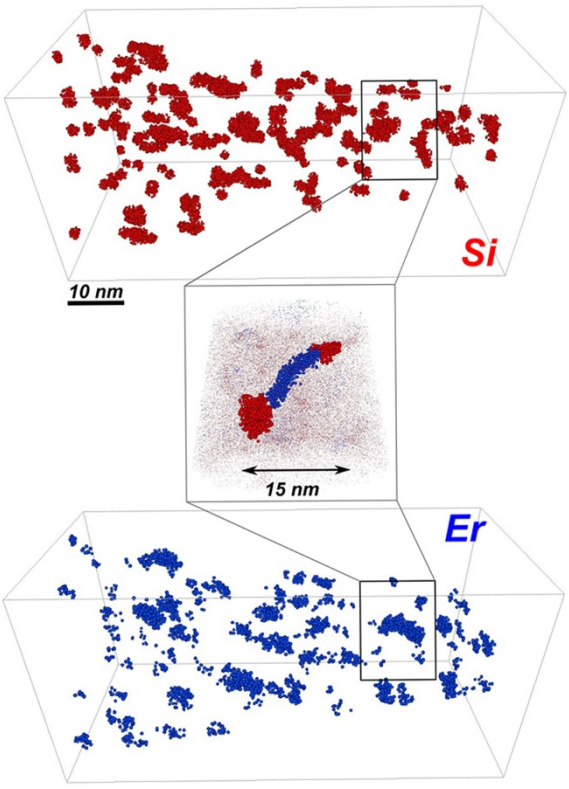

Figure 4 3D reconstruction of the annealed Er-doped SRSO layers of APT analysis. 3D cluster-filtered distributions of chemical species (Si in red and Er in blue) in Er-doped SRSO layers annealed at 1,100°C for 1 h. For clarity, only silicon and erbium atoms which belong to clusters are represented. Two Si-ncs linked by Er-rich aggregates are shown in the inset.

light, the total number of Si sensitizers decreases due to the merging of several small Si sensitizers along with the increase of Si-to-Er distance.

The measurement of the clusters' composition, which can be difficult in APT volume, has been performed using the procedure developed by Vurpillot et al. [30] and was recently applied by Talbot et al. on similar Si nanostructured materials [18,25]. The size distribution of the Si-ncs is well fitted by a Gaussian law. The minimum and maximum observed radii are 0.9 ± 0.3 and 2.3 ± 0.3 nm, respectively, whereas the mean radius of Si-ncs was estimated to be $< r >= 1.3 \pm 0.3$ nm. Along with this, about 50% of Si-ncs have the radii in the range of 1.0 to 1.5 nm. The volume fraction of Si clusters is given by the following formula:

$$f_V^{\mathrm{Si}} = \frac{C_{\mathrm{Si}}^0 - C_{\mathrm{Si}}^M}{C_{\mathrm{Si}}^C - C_{\mathrm{Si}}^M}, \quad (1)$$

where C_{Si}^C, C_{Si}^0, and C_{Si}^M are the compositions of Si in the Si-pure clusters, in the whole sample and in the matrix, respectively. The compositions have been extracted from

the concentration (in at.%) using the density of pure Si ($d_{Si} = 5.0 \times 10^{22}$ at./cm^3) and pure silica ($d_{SiO_2} = 6.6 \times 10^{22}$ at./cm^3); $f_V^{Si} = 4.0\%$ is obtained from Equation 1.

The Si diffusion coefficient has been deduced from the Einstein equation of self-diffusivity: $< \rho >= \sqrt{6Dt}$, where $< \rho >$ is the average displacement in three dimensions, t is the diffusion time, and D is the diffusion coefficient. The average displacement $< \rho >$ was estimated as the mean distance between the surfaces of two first- neighbor Si-ncs. The Si diffusion coefficient at 1,100°C, deduced from our data ($< \rho >= 4.3$ nm and $t = 3,600$ s) is equal to $D_{Si} = 8.4 \times 10^{-18}$ cm^2/s. Such a value is close to the silicon diffusion coefficient measured in Si-implanted SiO_2 materials ($D_{Si} = 5.7 \times 10^{-18}$ cm^2/s) obtained by Tsoukalas et al. [31,32]. As far as the Er-rich clusters are concerned, we have reported all the measured compositions of individual cluster on the ternary phase diagram Si-O-Er (Figure 5). This figure clearly illustrates that the composition of Er-rich clusters deals with a non-equilibrium phase in comparison with $ErSi_2$, Er_2Si_5, or Er_2O_3 expected from the binary equilibrium phase diagram of Er-Si and Er-O. Moreover, the present results are consistent with those of Xu et al. [33] and Kashtiban et al. [34], who have showed the absence of the mentioned Er equilibrium compounds in similar Er-doped Si-rich SiO_2 materials. The mean composition of Er-rich clusters is $X_{Er}^C = 11.9 \pm 0.4$ at.%, $X_O^C = 59.7 \pm 0.4$ at.% and $X_{Si}^C = 28.4 \pm 0.4$ at.% which corresponds to the $ErSi_3O_6$ phase. This result is also in agreement with similar $ErGe_XO_Y$ amorphous clusters observed recently by Kanjilal et al. by HRTEM [35]. The volume fraction (f_V^{Er}) and atomic fraction (f_a^{Er}) of Er atoms in the clusters are given by the following formula (assuming the same density between Er-rich clusters and silica matrix):

$$f_V^{Er} = \frac{C_{Er}^0 - C_{Er}^M}{C_{Er}^C - C_{Er}^M}, \tag{2}$$

$$f_a^{Er} = \frac{C_{Er}^C}{C_{Er}^0}\left(\frac{C_{Er}^0 - C_{Er}^M}{C_{Er}^C - C_{Er}^M}\right), \tag{3}$$

where C_{Er}^C, CX_{Er}^0 and C_{Er}^M are the compositions of Er in the Er-rich clusters, in the whole sample and in the matrix, respectively. Following Equations 2 and 3 , the atomic and volume fractions are estimated to be $f_a^{Er} = 30\%$ and $f_V^{Er} = 4.8\%$. This indicates that after annealing, about 70% of the total Er amount remains in solid solution as 'isolated' atoms, whereas the rest (30%) of Er^{3+} ions belongs to Er-rich clusters. We should note that the content of Er atoms, detected in our sample after 1,100°C annealing step, exceeds the solubility limit of Er in SiO_2, estimated as 0.1 at.% ($< 10^{20}$ at/cm^3) [36,37]. This explains the decrease in the Er^{3+} PL emission noticed in this film (Figure 1) after such a high-temperature annealing treatment similar to that reported in another work [29]. Moreover, we can note that the decrease of the PL intensity is higher than expected if only 30% of the Er amount is located in Er-rich clusters. To explain such a decrease, we assume that annealing treatment leads to the Si-nc density decreases (while Si-nc size increases) and the increase of Si-nc-Er interaction distance as well as to the decrease of the number of optically active Er ions coupled with Si-ncs.

The 3D chemical maps also indicate that the Er-rich clusters are likely formed in the vicinity of Si-ncs upon an annealing stage. This fact can be attributed to a preferential segregation of Er atoms at the Si-ncs/matrix interface during the phase separation process, similar to the results reported by Crowe et al. [38]. However, this hypothesis is not supported by the results of Pellegrino et al. [11], who concluded to a preferential segregation of Er in poor Si-nc region. In their paper, a double-implantation annealing process was applied to fabricate an Er-doped SRSO layer. This double process may stimulate Er diffusion explaining the segregation of Er and Si during the different implantation stages, which is contrary to our case.

Based on the hypothesis of spherical radius and on the determination of an amount of Er, Si, and O atoms in Er-rich clusters detected by APT method, the mean Er-rich cluster radius is estimated to be 1.4 ± 0.3 nm in the sample annealed at 1,100°C ($< \rho >= 5.1$ nm and $t = 3,600$ s). Erbium diffusion coefficient in the SRSO layer has been deduced using the Einstein equation of self-diffusivity. It has been found to be $D_{Er} \approx 1.2 \times 10^{-17}$ cm$^2 \cdot$ s^{-1} at 1,100°C. This value is about one order of magnitude lower than that reported by Lu et al. (4.3×10^{-16} cm$^2 \cdot$ s^{-1}) [39]

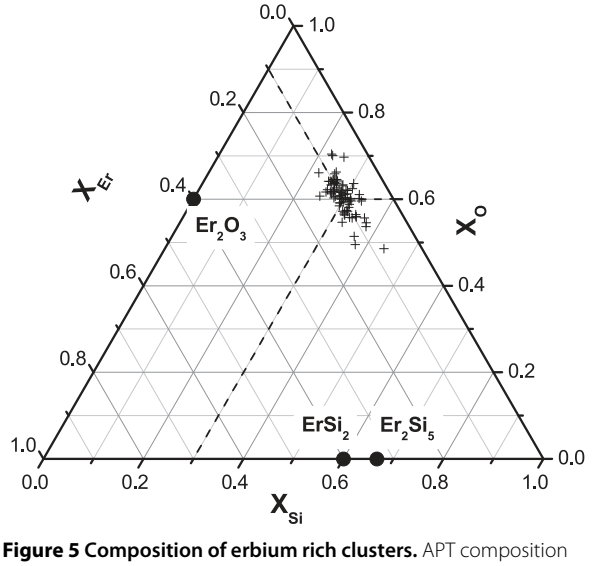

Figure 5 Composition of erbium rich clusters. APT composition measurements of individual Er-rich clusters compositions reported in the ternary Si-O-Er phase diagram.

which has been measured in SiO_2. This difference could be attributed to the presence of Si excess in the film.

The formation of Er-rich clusters explains the evolution of the optical properties of Er-doped layers upon high-temperature annealing treatment applied [12,13,29]. It is worth to note that the fabrication approach, chemical composition, and microstructure of initial samples define strongly the effect of post-annealing processing.

Conclusions

In this paper, the first investigation by APT, to our knowledge, of the nanostructure of Er-doped silicon-rich silica layer was performed at the atomic level and correlated with photoluminescence properties. The phase separation process between Si excess and the surrounding matrix was studied, and a formation of Si-rich or Er-rich phases was observed for samples annealed at high-temperature (1,100°C). The Si excess atoms precipitate in the form of pure Si nanoclusters in the silica matrix. Simultaneously, Er atoms form Er-rich clusters (about 30% of total amount), whereas 70% of the total Er atoms are free-dispersed in the host, demonstrating a super-saturation state but with an increase of the Si-ncs-to-Er distances. The Er-rich clusters have complex shape and composition. They are localized at the Si-nc/matrix interface or in poor Si-nc regions, indicating a complicated precipitation mechanism. Diffusion coefficients for Si and Er have been deduced from APT experiments. We have directly evidenced the clustering of rare-earth ions upon high-temperature annealing in Er-doped Si-rich SiO_2 films. This process has been often expected but, to our knowledge, never observed and demonstrated directly for these materials fabricated by different techniques. These results evidence the critical point to monitor the microstructure of Er-doped SRSO layers for the required inversion of 50% of the Er concentration to achieve a net gain in future Er-doped amplifier device.

Competing interests

The authors declare that they have no competing interests.

Authors' contributions

ET and RL carried out the APT sample preparation by SEM-FIB and performed the atom probe analysis and data treatment. ET, LK, and FG wrote the paper. FG, LK, and KH fabricated the sample under investigation and carried out the optical measurements. PP supervised the study and made significant contributions to the structural properties. All authors read and approved the final manuscript.

Acknowledgements

This work was supported by the Upper Normandy Region and the French Ministry of Research in the framework of Research Networks of Upper Normandy.

Author details

[1]Groupe de Physique des Matériaux (GPM), Université et INSA de Rouen, UMR CNRS 6634, Normandie Université, Av. de l'Université, BP 12, Saint Etienne du Rouvray, 76801, France. [2]Centre de Recherche sur les Ions, les Matériaux et la Photonique (CIMAP), CEA/CNRS/ENSICAEN/UCBN, 6 Bd. Maréchal Juin, Caen Cedex 4, 14050, France.

Received: 4 October 2012 Accepted: 19 November 2012
Published: 21 January 2013

References

1. Fujii M, Yoshida M, Kanzawa Y, Hayashi S, Yamamoto K: **1.54 μm photoluminescence of Er^{3+} doped into SiO_2 films containing Si nanocrystals: evidence for energy transfer from Si nanocrystals to Er^{3+}.** *Appl Physics Lett* 1997, **71**(9):1198.
2. Pacifici D, Irrera A, Franzo G, Miritello M, Iacona F, Priolo F: **Erbium-doped Si nanocrystals: optical properties and electroluminescent devices.** *Physica E: Low-dimensional Syst Nanostructures* 2003, **16**(3-4): 331–340.
3. Kenyon AJ, Trwoga PF, Federighi M, Pitt CW: **Optical properties of PECVD erbium-doped silicon-rich silica: evidence for energy transfer between silicon microclusters and erbium ions.** *J Phys: Condensed Matter* 1994, **6**(21):L319.
4. Kik PG, Brongersma ML, Polman A: **Strong exciton-erbium coupling in Si nanocrystal-doped SiO_2.** *App Phys Lett* 2325, **76**(17):2000.
5. Daldosso N, Luppi M, Ossicini S, Degoli E, Magri R, Dalba G, Fornasini P, Grisenti R, Rocca F, Pavesi L, Boninelli S, Priolo F, Spinella C, Iacona F: **Role of the interface region on the optoelectronic properties of silicon nanocrystals embedded in SiO_2.** *Phys Rev B* 2003, **68:**085327.
6. Ternon C, Dufour C, Gourbilleau F, Rizk R: **Role of interfaces in nanostructured silicon luminescence.** *Eur Phys J B* 2004, **41:**325.
7. Gourbilleau F, Madelon R, Dufour C, Rizk R: **Fabrication and optical properties of Er-doped multilayers Si-rich SiO_2/SiO_2: size control, optimum Er-Si coupling and interaction distance monitoring.** *Opt Mater* 2005, **27**(5):868–875.
8. Jhe JH, Shin JH, Kim KJ, Moon DW: **The characteristic carrier–Er interaction distance in Er-doped a-Si/SiO_2 superlattices formed by ion sputtering.** *Appl Phys Lett* 2003, **82**(25):4489.
9. Garrido B, Garcia C, Seo SY, Pellegrino P, Navarro-Urrios D, Daldosso N, Pavesi L, Gourbilleau F, Rizk R: **Excitable Er fraction and quenching phenomena in Er-doped SiO_2 layers containing Si nanoclusters.** *Physical Review B* 2007, **76**(24):245308.
10. Izeddin I, Moskalenko AS, Yassievich IN, Fujii M, Gregorkiewicz T: **Nanosecond dynamics of the near-infrared photoluminescence of Er-doped SiO_2 sensitized with Si nanocrystals.** *Phys Rev Lett* 2006, **97**(20):207401.
11. Pellegrino P, Garrido B, Arbiol J, Garcia C, Lebour Y, Morante JR: **Site of Er ions in silica layers codoped with Si nanoclusters and Er.** *Appl Phys Lett* 2006, **88**(12):121915.
12. Gourbilleau F, Levalois M, Dufour C, Vicens J, Rizk R: **Optimized conditions for an enhanced coupling rate between Er ions and Si nanoclusters for an improved 1.54-μm emission.** *J Appl Phys* 2004, **95**(7):3717.
13. Franzo G, Boninelli S, Pacifici D, Priolo F, Iacona F, Bongiorno C: **Sensitizing properties of amorphous Si clusters on the 1.54-μm luminescence of Er in Si-rich SiO_2.** *Appl Phys Lett* 2003, **82**(22):3871.
14. Bian LF, Zhang CG, Chen WD, Hsu CC, Shi T: **Local environment of Er^{3+} in Er-doped Si nanoclusters embedded in SiO_2 films.** *Appl Phys Lett* 2006, **89**(23):231927.
15. Maurizio C, D'Acapito F, Priolo F, Franzo G, Iacona F, Borsella E, Padovani S, Mazzoldi P: **Site of Er ions in Er-implanted silica containing Si nanoclusters.** *Opt Mater* 2005, **27**(5):900–903.
16. Noe P, Okuno H, Jager JB, Delamadeleine E, Demichel O, Rouvière JL, Calvo V, Maurizio C, D'Acapito F: **The evolution of the fraction of Er ions sensitized by Si nanostructures in silicon-rich silicon oxide thin films.** *Nanotechnology* 2009, **20**(35):355704.
17. Thogersen A, Mayandi J, Finstad T, Olsen A, Diplas S, Mitome M, Bando Y: **The formation of Er-oxide nanoclusters in SiO_2 thin films with excess Si.** *J Appl Phys* 2009, **106:**014305.
18. Talbot E, Lardé R, Gourbilleau F, Dufour C, Pareige P: **Si nanoparticles in SiO_2: An atomic scale observation for optimization of optical devices.** *EPL (Europhysics Lett)* 2009, **87**(2):26004.
19. Roussel M, Talbot E, Gourbilleau F, Pareige P: **Atomic characterization of Si nanoclusters embedded in SiO_2 by atom probe tomography.** *Nanoscale Res Lett* 2011, **6:**164.
20. Larson DJ, Foord DT, Petford-Long AK, Liew H, Blamire MG, Cerezo A, Smith GDW: **Field-ion specimen preparation using focused ion-beam milling.** *Ultramicroscopy* 1999, **79**(1-4):287–293.

21. Hijazi K, Khomenkova L, Gourbilleau F, Cardin J, Rizk R: **Enhanced fraction of coupled Er in silicon-rich silicon oxide layers grown by magnetron co-sputtering.** *J Luminescence* 2009, **129**(12):1886–1889.
22. Cerezo A, Godfrey TJ, Smith GDW: **Application of a position-sensitive detector to atom probe microanalysis.** *Rev Sci Instrum* 1988, **59**(6):862.
23. Blavette D, Bostel A, Sarrau JM, Deconihout B, Menand A: **An atom probe for three-dimensional tomography.** *Nature* 1993, **363:**432–435.
24. Gault B, Vurpillot F, Vella A, Gilbert M, Menand A, Blavette D, Deconihout B: **Design of a femtosecond laser assisted tomographic atom probe.** *Rev Sci Instrum* 2006, **77**(4):043705.
25. Talbot E, Roussel M, Genevois C, Pareige P, Khomenkova L, Portier X, Gourbilleau F: **Atomic scale observation of phase separation and formation of silicon clusters in Hf high-κ silicates.** *J Appl Phys* 2012, **111**(10):103519.
26. Cadel E, Vurpillot F, Larde R, Duguay S, Deconihout B: **Depth resolution function of the laser assisted tomographic atom probe in the investigation of semiconductors.** *J Appl Phys* 2009, **106**(4):044908.
27. Cadel E, Barreau N, Kessler J, Pareige P: **Atom probe study of sodium distribution in polycrystalline Cu(In,Ga)Se_2 thin film.** *Acta Materialia* 2010, **58**(7):2634–2637.
28. Lardé R, Talbot E, Pareige P, Bieber H, Schmerber G, Colis S, Pierron-Bohnes V, Dinia A: **Evidence of superparamagnetic Co clusters in pulsed laser deposition-grown $Zn_{0.9}Co_{0.1}O$ thin films using atom probe tomography.** *J Am Chem Soc* 2011, **133**(5):1451–1458.
29. Hijazi K, Rizk R, Cardin J, Khomenkova L, Gourbilleau F: **Towards an optimum coupling between Er ions and Si-based sensitizers for integrated active photonics.** *J Appl Phys* 2009, **106**(2):024311.
30. Vurpillot F, Bostel A, Blavette D: **Trajectory overlaps and local magnification in three-dimensional atom probe.** *Appl Phys Lett* 2000, **76**(21):3127–3129.
31. Tsoukalas D, Tsamis C, Normand P: **Diffusivity measurements of silicon dioxide layers using isotopically pure material.** *J Appl Phys* 2001, **89:**7809.
32. Tsoukalas D, Tsamis C, Normand P: **Use of isotopically pure silicon material to estimate silicon diffusivity in silicon dioxide.** *Mater Res Soc Symp Proc* 2001, **669:**J.3.7.1.
33. Xu F, Xiao Z, Cheng G, Yi Z, Zhang T, Gu L, Wang X: **Erbium-doped silicon-rich silicon dioxide/silicon thin films fabricated by metal vapour vacuum arc ion source implantation.** *J Phys: Condensed Matter* 2002, **14**(3):L63–L69.
34. Kashtiban RJ, Bangert U, Crowe I, Halsall MP, Sherliker B, Harvey AJ, Eccles J, Knights AP, Gwilliam R, Gass M: **Structural and compositional study of erbium-doped silicon nanocrystals by HAADF , EELS and HRTEM techniques in an aberration corrected STEM.** *J Phys: Conf Series* 2009, **209:**012043.
35. Kanjilal A, Rebohle L, Voelskow M, Skorupa W, Helm M: **Defect-engineered blue-violet electroluminescence from Ge nanocrystal rich SiO_2 layers by Er doping.** *J Appl Phys* 2009, **106**(2):026104.
36. Polman A, Jacobson DC, Eaglesham DJ, Kistler RC, Poate JM: **Optical doping of waveguide materials by MeV Er implantation.** *J Appl Phys* 1991, **70**(7):3778.
37. Sckerl MW, Guldberg-Kjaer S, Rysholt Poulsen, M, Shi P, Chevallier J: **Precipitate coarsening and self organization in erbium-doped silica.** *Phys Rev B* 1999, **59**(21):13494.
38. Crowe IF, Kashtiban RJ, Sherliker B, Bangert U, Halsall MP, Knights AP, Gwilliam RM: **Spatially correlated erbium and Si nanocrystals in coimplanted SiO_2 after a single high temperature anneal.** *J Appl Phys* 2010, **107**(4):044316.
39. Lu YW, Julsgaard B, Petersen MC, Jensen RVS, Pedersen TG, Pedersen K, Larsen AN: **Erbium diffusion in silicon dioxide.** *Appl Phys Lett* 2010, **97**(14):141903.

doi:10.1186/1556-276X-8-39
Cite this article as: Talbot *et al.*: Nanoscale evidence of erbium clustering in Er-doped silicon-rich silica. *Nanoscale Research Letters* 2013 **8**:39.